

# Synthesis, characterization and anti-fouling properties of poly(ethylene glycol) grafted poly(vinylidene fluoride) copolymer membranes

Peng Wang,<sup>a</sup> K. L. Tan,<sup>a</sup> E. T. Kang<sup>\*b</sup> and K. G. Neoh<sup>b</sup>

<sup>a</sup>Department of Physics, National University of Singapore, Kent Ridge, Singapore 119260

<sup>b</sup>Department of Chemical Engineering, National University of Singapore, Kent Ridge, Singapore 119260. E-mail: cheket@nus.edu.sg; Fax: (65) 779-1936

Received 8th September 2000, Accepted 9th November 2000

First published as an Advance Article on the web 29th January 2001

Methoxypoly(ethylene glycol) monomethacrylate (PEGMA) graft-copolymerized poly(vinylidene fluoride) (PVDF) (the P(PEGMA)-*graft*-PVDF copolymer) was synthesized. The PVDF homopolymer in *N*-methyl-2-pyrrolidone (NMP) solution was first pretreated with ozone and the peroxide content of the ozone-treated PVDF was determined by assaying with 2,2-diphenyl-1-picrylhydrazyl (DPPH). The activated PVDF was then subjected to graft copolymerization with the PEGMA macromonomer in NMP. The microstructures and compositions of the P(PEGMA)-*graft*-PVDF copolymers were characterized by FT-IR, X-ray photoelectron spectroscopy (XPS), elemental analysis, differential scanning calorimetry (DSC) and thermogravimetric (TG) analysis. Ultra-filtration (UF) membranes were prepared from the P(PEGMA)-*graft*-PVDF copolymer by the phase-inversion method. The bulk and the surface compositions of the membranes were determined by elemental analysis and XPS, respectively. In general, the graft concentration increases with the PEGMA macromonomer concentration. Angle-resolved XPS analyses of the UF membranes prepared from the copolymer revealed a substantial surface enrichment of the hydrophilic PEGMA component. The morphology of the membranes was studied using scanning electron microscopy (SEM). The UF membrane prepared from the P(PEGMA)-*graft*-PVDF copolymer with a graft concentration ([PEGMA]/[CH<sub>2</sub>CF<sub>2</sub>] ratio) above 0.06 was effective in preventing bovine serum albumin (BSA) adsorption.

## Introduction

Poly(vinylidene fluoride) (PVDF) membranes are widely used in microfiltration (MF) and ultrafiltration (UF) due to their excellent chemical resistance, well-controlled porosity and good thermal properties.<sup>1</sup> However, filtration of protein-containing solutions using the traditional hydrophobic polymer membranes is strongly limited by the problem of fouling that occurs both on the membrane surface and within the pores. The issues of membrane fouling and the approaches commonly used to modify polymer membrane surfaces have been reviewed recently.<sup>2</sup> Fouling will lead to the decrease in permeate fluxes with time. As a result, the cleaning and replacement of the membrane account for a large percentage of the total water treatment cost.

Several methods to confer anti-fouling properties on the conventional hydrophobic membrane have therefore been investigated. Generally, they can be classified into coating and grafting techniques. In the former method, the membrane is dipped in a solution containing polymers that exhibit anti-fouling properties.<sup>3,4</sup> Covalent immobilization of hydrophilic species on the surfaces of membranes can be achieved by surface graft copolymerizations of the membrane with monomers or macromonomers in solutions.<sup>5-9</sup> Prior to the graft copolymerization process, the membrane has to be exposed to a gas plasma, ozone, or UV to introduce reactive groups on the membrane surface. Both the coating and the grafting techniques suffer from one of the following shortcomings.<sup>2</sup> First of all, the coated surface layers are readily susceptible to removal, especially by changes in solution pH. Secondly, surface grafting is usually accompanied by changes in membrane pore size distribution, leading to reduced permeability. Finally, these surface modification techniques impart

hydrophilicity mainly to the membrane surface, while fouling occurs not only on the membrane surface but also within the pore channels of the membranes.<sup>10,11</sup>

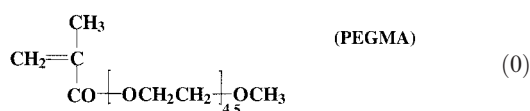
An appealing alternative might be the use of bulk-modified or chain-modified polymer as the membrane fabrication material. Poly(ethylene glycol) is well-known for its extraordinary ability to resist protein adsorption. This property is believed to result from its hydrophilicity, large excluded volume, and unique coordination with surrounding water molecules in an aqueous medium.<sup>12</sup> Surface-grafted PEG has rendered UF membranes resistant to oil and protein fouling.<sup>7</sup> Protein-resistant PVDF membranes have also been prepared from the self-organizing blends of an amphiphilic comb polymer, which has a poly(methacrylate) backbone and PEG side chains, in PVDF.<sup>2</sup> In the present work, we report the synthesis and characterization of PVDF with graft-copolymerized PEG side chains. The copolymer is shown to be a promising material for fabricating UF membranes with hydrophilic and anti-fouling properties.

## Experimental

### Materials

Poly(vinylidene fluoride) (PVDF, Kynar<sup>®</sup> K-761) powders having a molecular weight of 441000 were used in this study and were obtained from Elf Atochem North America Inc. Reagent grade *N*-methyl-2-pyrrolidone (NMP) was obtained from Merck Chem. Co. and was used as a solvent for the ozone treatment and graft copolymerization. Methoxypoly(ethylene glycol) monomethacrylate (PEGMA) macromonomer with a molecular weight of about 300 and *N,N*-dimethylacetamide (DMAc) for preparing the membrane casting solution were

obtained from Aldrich Chemical Co. (Milwaukee, WI). They were used without further purification. The chemical structure of the PEGMA macromonomer, with an average number of ethylene glycol units of about 4.5, is shown below.



### Ozone treatment

The PVDF powders were dissolved in NMP to a concentration of  $75 \text{ g L}^{-1}$ . A continuous stream of  $\text{O}_3\text{-O}_2$  mixture was bubbled through the solution at  $25^\circ\text{C}$ . The  $\text{O}_3\text{-O}_2$  mixture was generated from an Azcozon RMU16-04EM ozone generator. The gas flow rate was adjusted to  $300 \text{ L h}^{-1}$  to give rise to an ozone concentration of about  $0.027 \text{ g L}^{-1}$  in the gaseous mixture. The treatment time was varied from 15–30 min to achieve the desired content of peroxides. After the ozone treatment, the polymer solution was cooled quickly in an ice bath and the PVDF polymer was precipitated in excess ethanol. The solution was filtered and the ozone-treated PVDF was dried under reduced pressure at ambient temperature.

### Determination of peroxide concentration

An ozone-treated PVDF sample of about 150–200 mg was dissolved in 20 mL of NMP containing 12 mg of 2,2-diphenyl-1-picrylhydrazyl (DPPH). The solution was saturated with argon by bubbling the purified argon gas through it for 45 min. The reaction mixture was then placed in a thermostated oil bath at  $110^\circ\text{C}$  for 10 min. The reaction mixture was subsequently cooled in an ice bath. The ozone-treated polymer was precipitated with 160 mL of pure propan-2-ol. After 30 min, the solution was filtered and the residual DPPH concentration was determined by colorimetry at 520 nm. The number of moles of peroxides per gram of the ozone-treated PVDF ( $T$ ) can be determined from eqn. (1).<sup>13</sup>

$$T = ((C_0 - C) \times 180) / (2000 \times 394.33 \times m) \quad (1)$$

where  $C_0$  and  $C$  are the initial and final DPPH concentrations in  $\text{g L}^{-1}$ , respectively, and  $m$  is the weight of PVDF sample in g.

### Graft copolymerization of PVDF with PEGMA macromonomer: the P(PEGMA)-graft-PVDF copolymer

About 2 g of the ozone-pretreated PVDF was dissolved in 25 mL of NMP. The PVDF solution and the PEGMA macromonomer were introduced into a 3-necked flask equipped with a thermometer, a condenser, and a gas line. The macromonomer concentrations were varied from 50 to  $300 \text{ g L}^{-1}$ . The final volume of each reaction mixture was adjusted to 40 mL. The solution was saturated with purified argon for 30 min under constant stirring. The reactor flask was then placed in a thermostated oil bath at  $100^\circ\text{C}$ . An argon flow was maintained throughout the thermal graft copolymerization process. After the desired reaction time, the reactor flask was cooled in an ice bath and the P(PEGMA)-graft-PVDF copolymer was precipitated in excess ethanol (a good solvent for PEGMA homopolymer). After filtration, the P(PEGMA)-graft-PVDF was re-dissolved in 40 mL of acetone and then reprecipitated in 200 mL of ethanol. The above procedure was repeated twice. The graft-copolymerized PVDF sample was further purified by an equal volume mixture of methanol and acetone in a Soxhlet extractor for 24 h to remove any residual PEGMA homopolymers. The graft yields were typically in the range of 7 to 9%, based on the bulk composition analysis of the graft copolymer and by assuming that the non-grafted PEGMA units existed as the homopolymer. The ozone-

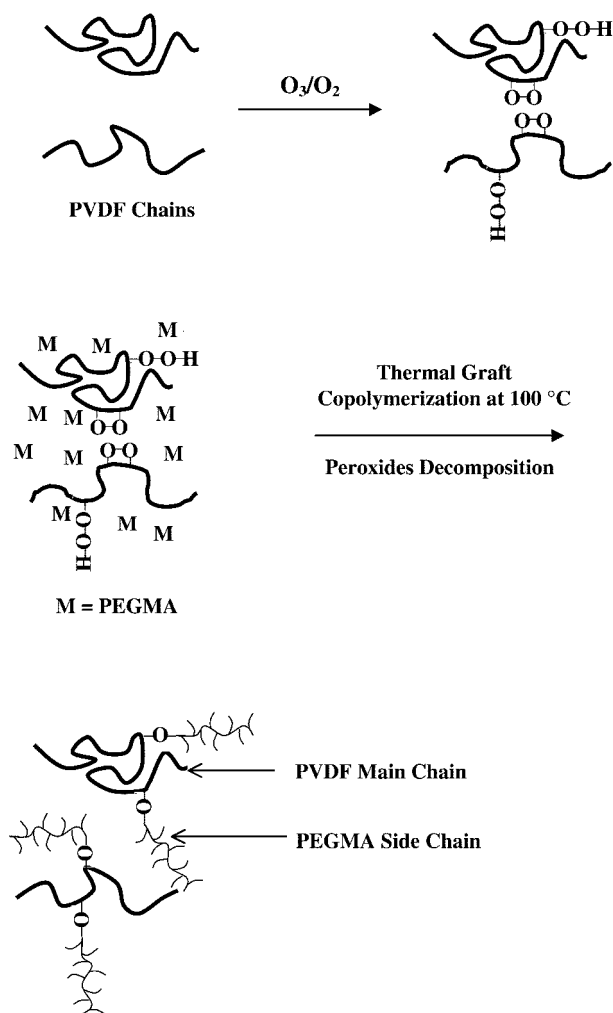


Fig. 1 Schematic representation of thermally induced graft copolymerization of PEGMA on to the ozone-activated PVDF backbone.

treatment step and the thermal graft copolymerization of PVDF with PEGMA are shown schematically in Fig. 1.

### Infrared spectroscopy

FT-IR spectra of thin polymer films cast from acetone solutions were obtained using a Bio-Rad FTS 135 FT-IR spectrophotometer. Each spectrum was collected by accumulating 16 scans at a resolution of  $8 \text{ cm}^{-1}$ .

### XPS measurements

X-Ray photoelectron spectroscopy (XPS) measurements were made on a VG ESCALAB MkII spectrometer with a  $\text{Mg-K}\alpha$  X-ray source (1253.6 eV photons) at a constant retard ratio of 40. The polymer films and membranes were mounted on the standard sample studs by means of double-sided adhesive tape. The core-level signals were obtained at the photoelectron take-off angles ( $\alpha$ , with respect to the sample surface) of  $20^\circ$  and  $75^\circ$ . The X-ray source was run at a reduced power of 120 W. The pressure in the analysis chamber was maintained at  $7.5 \times 10^{-9}$  Torr or lower during each measurement. All binding energies (BE's) were referenced to the C1s neutral carbon peak at 284.6 eV or the  $\text{CF}_2$  peak of PVDF at 290.5 eV. In peak synthesis, the line width (full width at half-maximum, or FWHM) for the Gaussian peaks was maintained constant for all components in a particular spectrum. Surface elemental stoichiometries were determined from peak-area ratios, after correcting with the experimentally determined sensitivity factors, and were reliable to  $\pm 10\%$ . The elemental sensitivity

factors were determined using stable binary compounds of well-established stoichiometries.

### Water contact angle measurements

The static water contact angles of PVDF thin films cast from acetone solutions of pristine and ozone-treated PVDF samples were measured at 25 °C and 60% relative humidity using a sessile drop method in a telescopic goniometer (Rame-Hart Model 100-00(230)). The telescope with a magnification power of 23× was equipped with a protractor of 1° graduation. For each angle reported, at least five sample readings from different surface locations were averaged. The angles reported were reliable to ±3°.

### Elemental analyses

Elemental analyses of the copolymer samples were performed by the Microanalysis Centre of the National University of Singapore. The bulk C and H atomic ratios were determined on a Perkin-Elmer 2400 elemental analyzer. The F content was determined, on the other hand, by the Schöniger combustion method.<sup>14</sup>

### Thermal analyses

The thermal properties of the copolymers were determined using both differential scanning calorimetry (DSC) and thermogravimetric (TG) analysis. For the DSC measurements, the melting temperatures were obtained at a heating rate of 10 °C min<sup>-1</sup> and under a dry nitrogen atmosphere in a Netzsch DSC-50 differential scanning calorimeter. For TG analysis, the polymer samples were heated up to 700 °C at a heating rate of 10 °C min<sup>-1</sup> under a dry nitrogen atmosphere in the Du Pont Thermal Analyst 2100 system, equipped with a TGA 2050 thermogravimetric thermal analyzer.

### UF membrane preparation

UF membranes were prepared by phase-inversion from solutions containing 15% (w/w) polymer or copolymer in *N,N*-dimethylacetamide (DMAc). The polymer or copolymer solution was cast onto a glass plate, which was immersed in a bath of doubly distilled water after the solution had been subjected to a brief period of evaporation in air. Each membrane was left in water for about 20 min after separation from the glass plate. It was then extracted in a second bath of doubly distilled water at 80 °C for 30 min. Such a heat-treatment step was commonly performed during the fabrication of commercial membranes in order to refine the pore size distribution.<sup>15</sup> The purified membranes were dried under reduced pressure for subsequent characterization.

### Morphology of the UF membranes

The surface morphology of the UF membranes was studied by scanning electron microscopy (SEM) using a JEOL 6320 electron microscope. The membranes were mounted on the sample studs by means of double-sided adhesive tape and were shadowed with gold prior to SEM measurements. The SEM

measurements were performed at an accelerating voltage of 8 kV.

### Protein adsorption

The protein, bovine serum albumin (BSA), was obtained from Sigma Chemical Co. (St. Louis, MO). The BSA was dissolved in the phosphate-buffered saline (PBS, pH=7.4) at the concentration of 2 mg mL<sup>-1</sup>. The UF membranes were rinsed initially with PBS to rehydrate the surface and then placed in the BSA solution. The adsorption was allowed to proceed at 25 °C for 24 h. The membranes were then removed from the solution, gently washed three times with PBS from a Pasteur pipette, and rinsed once with doubly distilled water to remove the PBS salt. After drying under reduced pressure, the protein-adsorbed surfaces were analyzed by X-ray photoelectron spectroscopy (XPS). The N1s core-level signal was used as a marker for the analysis of the protein adsorbed on the surface.<sup>16</sup>

## Results and discussion

### Ozone treatment of the PVDF polymer in solution

Ozone treatment of polymer as an activation step for grafting and graft copolymerization has been known for some time. Wang *et al.*<sup>17</sup> pretreated low-density polyethylene (LDPE) films with ozone to facilitate the surface grafting of hydrophilic polymers. The surfaces of conjugated polymers, such as polyaniline (PANi) and polypyrrole (PPY) films, have been modified by ozone treatment and graft copolymerization with acrylic acid (AAc).<sup>18</sup> Boutevin *et al.*<sup>19</sup> activated PVDF with ozone, followed by graft copolymerization with methyl methacrylate (MMA), to give rise to the P(MMA)-graft-PVDF copolymers. Fargere *et al.*,<sup>13</sup> on the other hand, studied the radical copolymerization of styrene initiated by an ozonized ethylene-vinyl acetate copolymer (EVA).

Generally, the amount of peroxides in polymers introduced by ozone treatment can be regulated by the treatment temperature, ozone concentration and treatment time.<sup>13</sup> In this study, the ozone-treatment temperature was kept at room temperature (25 °C) and the ozone concentration was fixed at 0.027 g L<sup>-1</sup> of the O<sub>3</sub>-O<sub>2</sub> mixture. The peroxides content of the ozone-treated PVDF samples (in mol per gram of the activated PVDF and determined from the DPPH assay) is shown in Table 1. It can be seen that the peroxides concentration increases with increasing ozone-treatment time. The increase in the peroxides concentration is also consistent with the corresponding increase in the elemental [O]/[C] ratio, as determined from the O1s and C1s XPS core-level spectral area ratio of the sample (Table 1). Ozone treatment of the PVDF polymer is accompanied by a small amount of polymer degradation, as indicated by the decrease in intrinsic viscosity (and thus molecular weight) of the solution (also shown in Table 1). The intrinsic viscosity data of the polymer solutions were obtained at 25 °C in NMP, using an Ostwald viscometer.

Ozone treatment can introduce certain polar groups, such as carbonyl and ketone groups into polymers.<sup>13</sup> Comparing the IR spectra of PVDF thin films cast from acetone solutions of

**Table 1** Peroxides content, intrinsic viscosity and water contact angle of pristine and ozone-treated PVDF

Sample	Peroxides content <sup>a</sup> (mol g <sup>-1</sup> of polymer)	[η] <sup>b</sup>	Water contact angle (°) of the film cast from acetone solution	[O]/[C] Ratio <sup>c</sup>
Pristine PVDF	0	1.63	133	0
5 min ozone-treated PVDF	5 × 10 <sup>-5</sup>	1.32	128	0.003
15 min ozone-treated PVDF	10 × 10 <sup>-5</sup>	1.17	120	0.007
30 min ozone-treated PVDF	13 × 10 <sup>-5</sup>	1.04	115	0.01

<sup>a</sup>Determined from reaction with DPPH. <sup>b</sup>Intrinsic viscosity at 25 °C in NMP. <sup>c</sup>Determined from the corrected O1s and C1s XPS core-level spectral area ratio of the respective sample (obtained at the photoelectron take-off angle, α, of 75°).

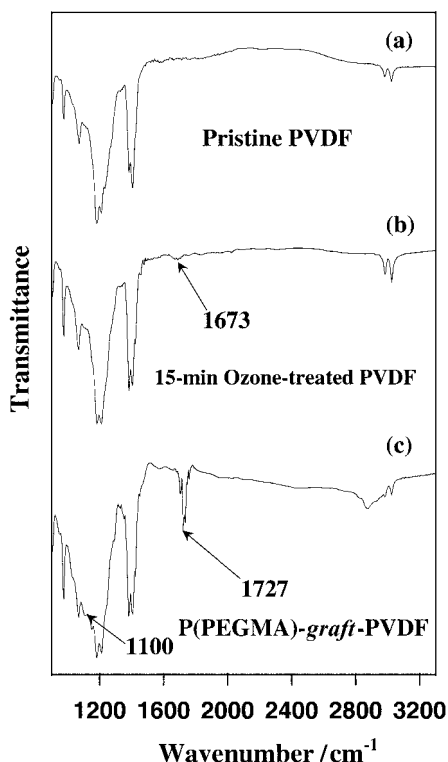


**Fig. 2** FT-IR spectra of (a) a pristine PVDF film, (b) the PVDF thin film cast from acetone solution of the 15 min ozone-treated sample, and (c) P(PEGMA)-*graft*-PVDF thin film cast from acetone solution (graft concentration or  $[C]/[F]_{\text{bulk}} = 1.44$ ).

pristine PVDF and PVDF with 15 min of ozone treatment (Fig. 2(a) and Fig. 2(b), respectively), a new peak at  $1673 \text{ cm}^{-1}$ , attributable to the carbonyl group, appears in the ozone-treated PVDF. In Table 1, the contact angle data suggest that the film cast from the ozone-treated PVDF becomes less hydrophobic than that cast from the pristine PVDF. The water contact angle of a pure dense PVDF film with smooth surface, obtained from Goodfellow Ltd. of Cambridge, UK, is about  $82^\circ$ . However, the contact angles observed in the present films are much higher. The large values of the contact angles are due to the high surface roughness of the porous films cast from acetone solutions. The extraordinary effect of surface roughness on the observed water contact angle has been discussed quantitatively by Good.<sup>20</sup>

#### Thermally induced graft copolymerization of PEGMA macromonomer

It has been reported by Boutevin *et al.*<sup>19,21</sup> that the activation energy and the Arrhenius coefficient of the initiators in the ozone-treated PVDF are  $39 \text{ kJ mol}^{-1}$  and 5.8, respectively. On the basis of these data, the half-life for the decomposition of peroxides on the ozone-treated PVDF was estimated to be about 10 min at  $100^\circ\text{C}$ . Thus, a polymerization time of 1.5 h at  $100^\circ\text{C}$  was sufficient for the complete decomposition of the peroxides introduced on to PVDF during ozone pretreatment. In the present study, gelation was observed for graft copolymerization times longer than 1.5 h in the presence of a high concentration of the PEGMA macromonomer (weight ratio of PEGMA : PVDF = 4 : 1 or higher).

The structure of the PEGMA graft-copolymerized PVDF (P(PEGMA)-*graft*-PVDF) polymer was studied by FT-IR and XPS. The FT-IR spectrum of a P(PEGMA)-*graft*-PVDF thin film (graft concentration or  $[C]/[F]_{\text{bulk}} = 1.44$ , see below) is shown in Fig. 2(c). The spectrum contains the characteristic band for the O–C=O stretch ( $\nu = 1727 \text{ cm}^{-1}$ ), attributable to the ester groups in the grafted PEGMA polymer, and the band

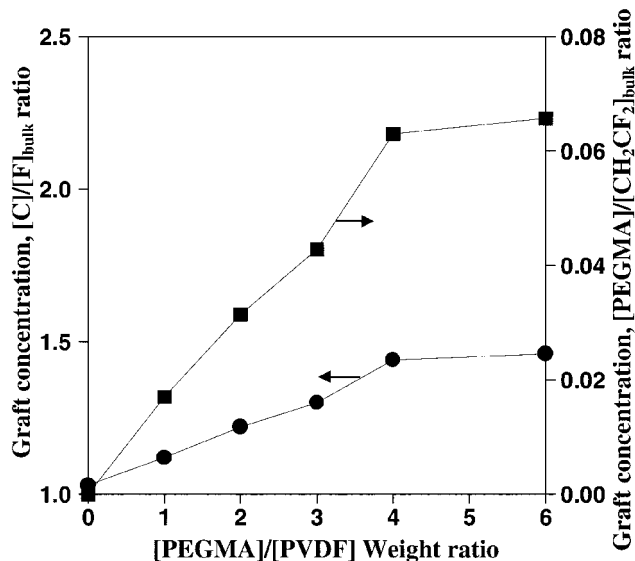


**Fig. 3** Effect of the macromonomer concentration on the bulk graft concentration of the PEGMA polymer.

for the C–O stretch ( $\nu = 1100 \text{ cm}^{-1}$ ), attributable to the ether groups of PEGMA.

The bulk graft concentration can be represented simply as the carbon to fluorine ratio, obtained from elemental analyses and by taking into account the fact that the PVDF substrate chain has a  $[C]/[F]$  ratio of 1.0. The graft concentration in terms of number of PEGMA repeat units per PVDF repeat unit, or the  $[\text{PEGMA}]/[\text{CH}_2\text{CF}_2]_{\text{bulk}}$  ratio can be obtained readily from the  $[C]/[F]_{\text{bulk}}$  ratio by taking into account the carbon stoichiometry of the graft chains and the carbon and fluoride stoichiometries of the substrate chains. Thus, the  $[\text{PEGMA}]/[\text{CH}_2\text{CF}_2]_{\text{bulk}}$  ratio can be calculated from eqn. (2).

$$[\text{PEGMA}]/[\text{CH}_2\text{CF}_2]_{\text{bulk}} = 2/14 \times ([C]/[F]_{\text{bulk}} - 1) \quad (2)$$

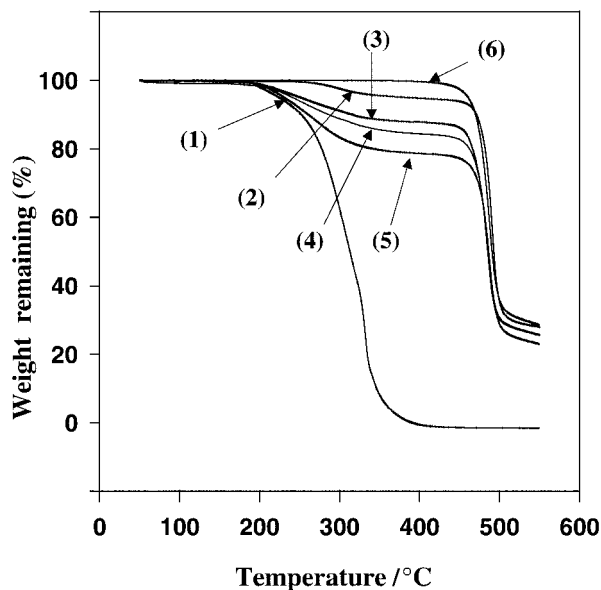
in which the factor 2/14 accounts for the fact that there are 2 and 14 carbons per repeat unit of PVDF and P(PEGMA), respectively.

Fig. 3 shows the dependence of the graft concentration of the PEGMA polymer, expressed as the  $[C]/[F]_{\text{bulk}}$  and  $[\text{PEGMA}]/[\text{CH}_2\text{CF}_2]_{\text{bulk}}$  ratios, on the PEGMA macromonomer concentration used for the thermally induced graft copolymerization. The ozone pretreatment time of the PVDF solution was fixed at 15 min and the thermally induced graft copolymerization time at 1.5 h. The graft concentration increases with increasing PEGMA macromonomer concentration used for graft copolymerization. The effect of the macromonomer concentration, however, levels off at a  $[\text{PEGMA}]/[\text{PVDF}]$  weight ratio greater than about 4 under the present graft copolymerization conditions.

#### Thermal analysis

The graft copolymers were analyzed by differential scanning calorimetry (DSC) and thermogravimetric (TG) analysis. Fig. 4 shows the respective TG analysis curves of the pristine PVDF homopolymer, the P(PEGMA)-*graft*-PVDF copolymers of various graft concentrations, and the PEGMA homopolymer. The PEGMA graft-copolymerized PVDF samples show intermediate weight loss behavior in comparison to that of the PEGMA homopolymer and that of PVDF. A distinct two-step degradation process is discernible for the copolymer samples. The onset of the first major weight loss at about  $200^\circ\text{C}$  corresponds to the decomposition of the P(PEGMA) component. The second major weight loss begins at about  $415^\circ\text{C}$ , corresponding to the decomposition of the PVDF polymer. The extent of the first major weight loss





**Fig. 4** TG analysis of (1) the PEGMA homopolymer, (2) P(PEGMA)-*graft*-PVDF (graft concentration or  $[C]/[F]_{\text{bulk}} = 1.12$ ), (3) P(PEGMA)-*graft*-PVDF (graft concentration or  $[C]/[F]_{\text{bulk}} = 1.22$ ), (4) P(PEGMA)-*graft*-PVDF (graft concentration or  $[C]/[F]_{\text{bulk}} = 1.30$ ), (5) P(PEGMA)-*graft*-PVDF (graft concentration or  $[C]/[F]_{\text{bulk}} = 1.44$ ), and (6) the pristine PVDF.

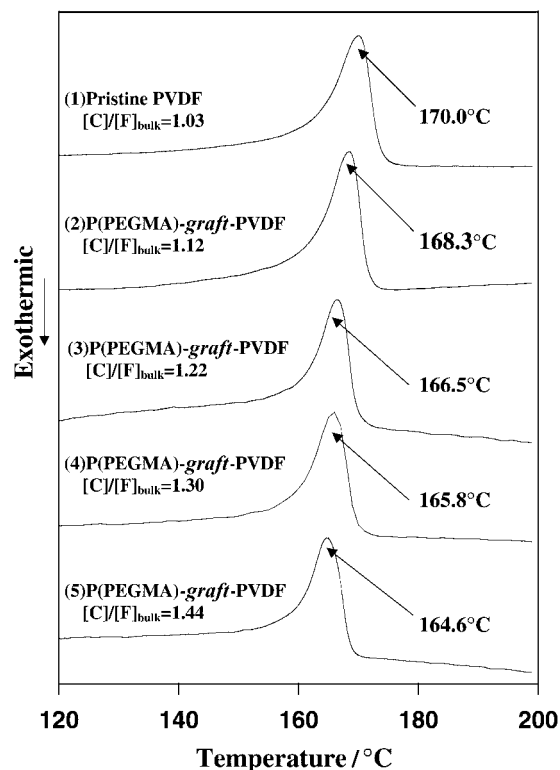
at about 200 °C coincides approximately with the P(PEGMA) content in the respective graft copolymer.

Fig. 5 shows the DSC curves of the pristine PVDF and the P(PEGMA)-*graft*-PVDF copolymers of various graft concentrations. It is well known that PVDF is a crystalline polymer arising from its highly symmetrical structure. It has a melting point of about 170 °C. As the melting temperature of a crystalline polymer is dependent on the sample history, the DSC curves in Fig. 5 were obtained from the second scans, after allowing the respective samples to anneal from the initial scans. After graft-copolymerization with PEGMA, the structural symmetry is partially destroyed, resulting in the lowering of the melting point. It can also be seen that with the increase in graft concentration, the melting point of the graft copolymer becomes lower.

#### Surface morphology and composition of the UF membrane prepared from P(PEGMA)-*graft*-PVDF

Micrographs (a)–(d) in Fig. 6 are SEM images obtained at a magnification of 20000 × for UF membranes cast by the phase-inversion technique at 25 °C from DMAc solutions of pristine PVDF and P(PEGMA)-*graft*-PVDF copolymers of three different graft concentrations. The membranes cast from the DMAc solutions of P(PEGMA)-*graft*-PVDF have a much more uniform pore size distribution and higher porosities than that cast from the pristine PVDF.

The surface compositions of the UF membranes prepared by the phase-inversion method were determined by XPS. Fig. 7(a)–(d) show the respective C1s core-level spectra, obtained at  $\alpha = 20^\circ$ , for the pristine PVDF membrane and the membranes prepared from P(PEGMA)-*graft*-PVDF of different graft concentrations. In the case of the pristine PVDF film, the C1s core-level spectra can be curve fitted with two peak components, with binding energies (BE's) at 285.8 eV for the CH<sub>2</sub> species and 290.5 eV for the CF<sub>2</sub> species.<sup>22</sup> The ratio for the two peaks is about 1.04, which is in good agreement with the structure of PVDF and the data reported in the literature.<sup>23</sup> The C1s core-level spectra of the P(PEGMA)-*graft*-PVDF membranes, on the other hand, are curve-fitted with five components using the following approaches. The two peak components of about equal intensities, with BE's at 285.8 eV



**Fig. 5** DSC curves of (1) the pristine PVDF, (2) P(PEGMA)-*graft*-PVDF (graft concentration or  $[C]/[F]_{\text{bulk}} = 1.12$ ), (3) P(PEGMA)-*graft*-PVDF (graft concentration or  $[C]/[F]_{\text{bulk}} = 1.22$ ), (4) P(PEGMA)-*graft*-PVDF (graft concentration or  $[C]/[F]_{\text{bulk}} = 1.30$ ), and (5) P(PEGMA)-*graft*-PVDF (graft concentration or  $[C]/[F]_{\text{bulk}} = 1.44$ ).

for the CH<sub>2</sub> species and at 290.5 eV for the CF<sub>2</sub> species, can be assigned, unambiguously, to the PVDF substrate chains. The components with BE's at 286.2 and 288.5 eV are assigned, respectively, to the CO and O–C=O species in the P(PEGMA)

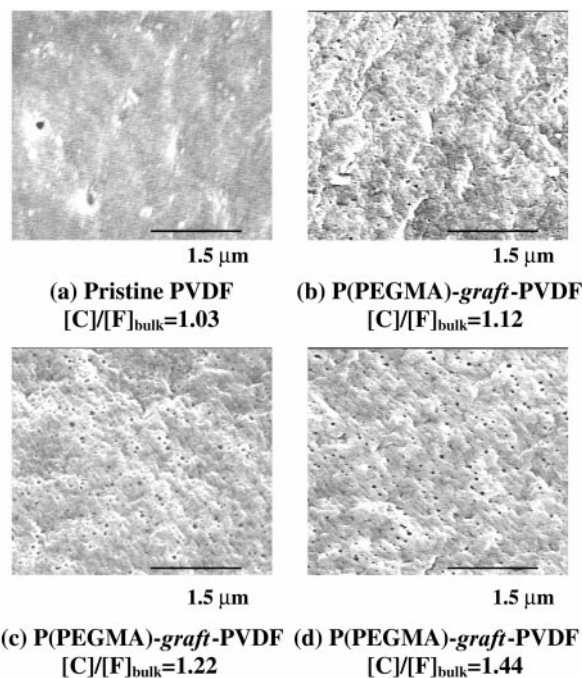


**Fig. 6** SEM micrographs of the surfaces of the UF membranes cast by phase inversion from 15% (w/w) DMAc solutions of (a) pristine PVDF, (b) P(PEGMA)-*graft*-PVDF (graft concentration or  $[C]/[F]_{\text{bulk}} = 1.12$ ), (c) P(PEGMA)-*graft*-PVDF (graft concentration or  $[C]/[F]_{\text{bulk}} = 1.22$ ), and (d) P(PEGMA)-*graft*-PVDF (graft concentration or  $[C]/[F]_{\text{bulk}} = 1.44$ ).

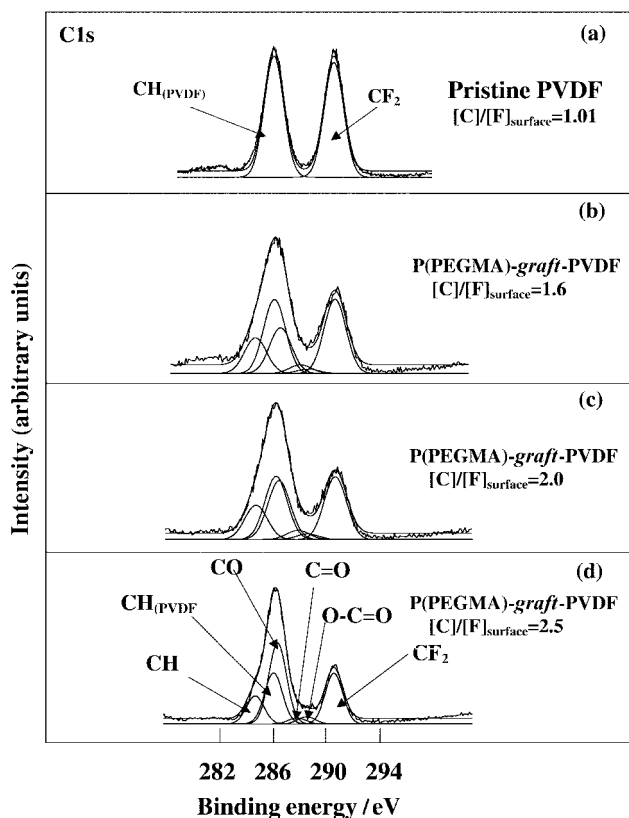


Fig. 7 XPS C1s core-level spectra and surface compositions, obtained at  $\alpha = 20^\circ$ , of the UF membranes prepared from: (a) the pristine PVDF ( $[C]/[F]_{\text{bulk}} \sim 1.03$ ) and the P(PEGMA)-*graft*-PVDF copolymers of: (b)  $[C]/[F]_{\text{bulk}} = 1.12$ , (c)  $[C]/[F]_{\text{bulk}} = 1.22$ , and (d)  $[C]/[F]_{\text{bulk}} = 1.44$ .

side chain.<sup>22</sup> The minor peak component with BE at 287.7 eV is attributable to the C=O species. The component with BE at 284.6 eV, on the other hand, is attributable to the neutral carbon in P(PEGMA) graft chain and, to a much lesser extent, the neutral carbon in the defluorinated PVDF backbone as a result of the ozone treatment.

The peak assignments are consistent with the surface graft concentration determined from the overall surface C and F analysis. Table 2 summarizes the surface graft concentrations

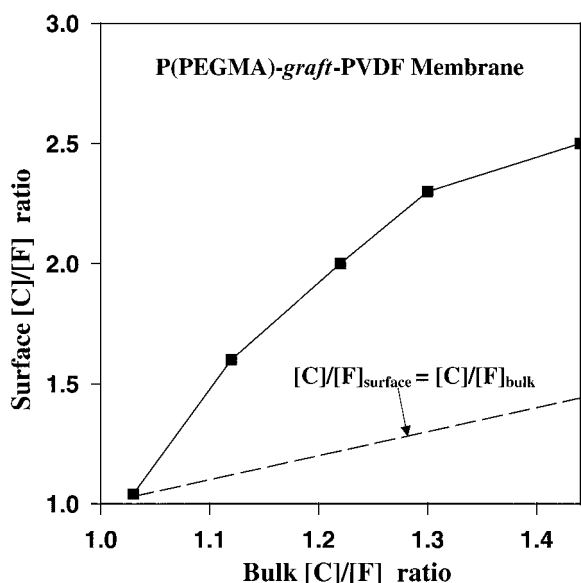


Fig. 8 Surface  $[C]/[F]$  ratio (determined by XPS at  $\alpha = 20^\circ$ ) versus bulk  $[C]/[F]$  ratio (determined by elemental analysis) of UF membranes cast from DMAc solutions of P(PEGMA)-*graft*-PVDF copolymers of different graft concentrations.

Table 2 Surface composition analysis of the P(PEGMA)-*graft*-PVDF UF membranes

Surface graft conc. $[C]/[F]_{\text{surface}}$	Surface graft conc. <sup>a</sup> $[PEGMA]/[CH_2CF_2]_{\text{surface}}$	XPS-derived $[CO]/[CF_2]$ ratio
1.01	0	0
1.6	0.08	0.66
2.0	0.14	0.98
2.3	0.18	1.46
2.5	0.21	1.68

<sup>a</sup>Based on the expression  $[PEGMA]/[CH_2CF_2]_{\text{surface}} = 2/14 \times ([C]/[F]_{\text{surface}} - 1)$  (see text).

of the various P(PEGMA)-*graft*-PVDF UF membranes. The XPS-derived  $[CO]/[CF_2]$  ratios, based on the peak analysis of Fig. 7, are also included in Table 2. The  $[CO]/[CF_2]$  ratio is related to the surface graft concentration, as the CO species is associated with the poly(ethylene glycol) side chain of the grafted P(PEGMA) while the  $CF_2$  species is associated with the repeat unit of the PVDF substrate. A good correlation between the increase in surface graft concentration ( $[PEGMA]/[CH_2CF_2]_{\text{surface}}$  ratio) and the  $[CO]/[CF_2]$  ratio is observed for the composition range studied (Table 2). Furthermore, each  $[CO]/[CF_2]$  ratio in Table 2 is about eight times that of the corresponding  $[PEGMA]/[CH_2CF_2]_{\text{surface}}$  ratio. This result is in good agreement with the fact that each PEGMA macromonomer contains, on average, four to five ethylene glycol units.

The surface  $[C]/[F]$  ratios (determined by XPS) versus the bulk  $[C]/[F]$  ratios (determined by elemental analysis) for UF membranes cast from DMAc solutions of P(PEGMA)-*graft*-PVDF of different graft concentrations are shown in Fig. 8. It can be seen that the surface  $[C]/[F]$  ratio is generally higher than the bulk  $[C]/[F]$  ratio. This phenomenon is due to the enrichment of the hydrophilic components from the grafted PEGMA polymers at the outermost surface during the course of the membrane formation by the phase-inversion method in an aqueous medium.

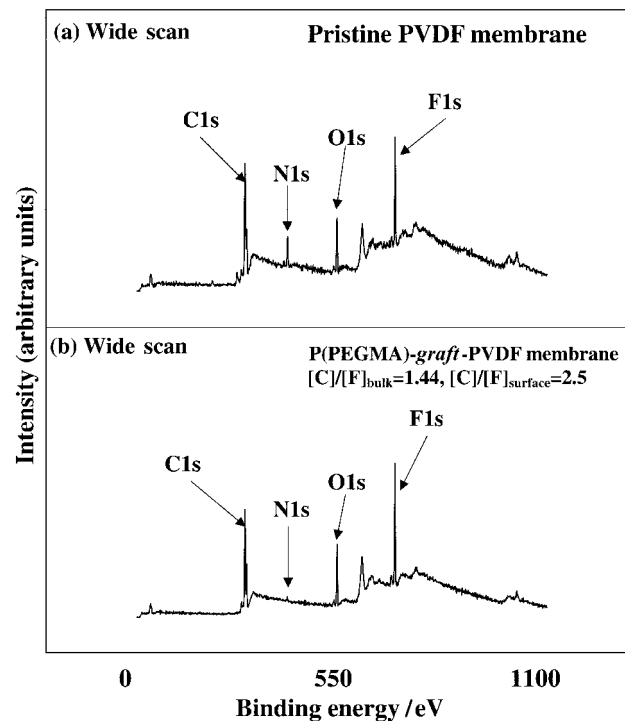


Fig. 9 XPS wide scan spectra of the UF membrane prepared from (a) the pristine PVDF and (b) P(PEGMA)-*graft*-PVDF (graft concentration or  $[C]/[F]_{\text{bulk}} = 1.44$ ) after exposure to a buffer solution containing  $2 \text{ mg mL}^{-1}$  BSA for 24 h.

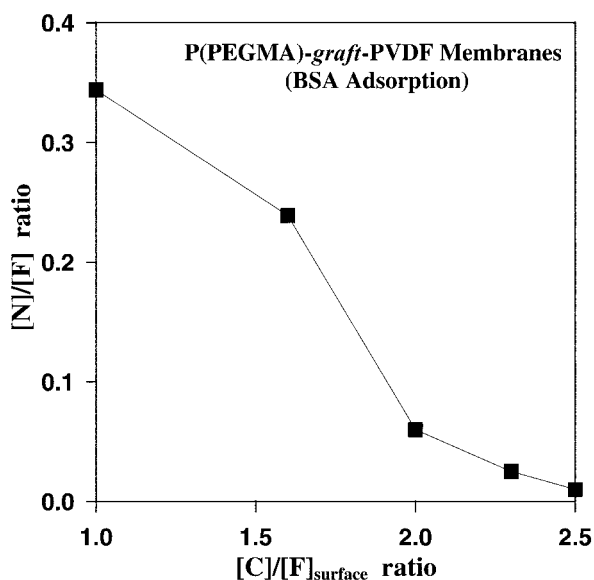


Fig. 10 Effect of P(PEGMA) graft concentration on the amount of BSA protein adsorbed on the surfaces of the UF membranes cast from P(PEGMA)-*graft*-PVDF copolymers of different graft concentrations.

### Protein adsorption characteristics

Bovine serum albumin (BSA) was allowed to adsorb on the pristine and the P(PEGMA)-*graft*-PVDF UF membrane surfaces. The relative amount of the protein adsorbed on each surface was derived from the XPS measurements. The nitrogen signal from the peptide bonds was used as a marker of the relative amount of protein adsorbed on the surface. Fig. 9 shows the XPS wide scan spectra of the surfaces of UF membranes prepared from pristine PVDF and P(PEGMA)-*graft*-PVDF (graft concentration or  $[C]/[F]_{\text{surface}} = 2.5$ ) after the protein adsorption in  $2 \text{ mg mL}^{-1}$  of BSA buffer solution for 24 h. The intensity of the N1s peak component (at the BE of about 400 eV) for the pristine PVDF membrane surface (Fig. 9(a)) is much higher than that for the P(PEGMA)-*graft*-PVDF membrane surface. Thus, a significantly larger amount of protein adsorption occurs on the pristine PVDF surface. This strong affinity of the pristine PVDF for BSA is probably due to the hydrophobic interaction of the protein molecules with the highly hydrophobic PVDF membrane surface.<sup>16</sup> For the P(PEGMA)-*graft*-PVDF (graft concentration or  $[C]/[F]_{\text{surface}} = 2.5$ ) membrane surface, the intensity of the nitrogen peak is fairly low. The relative amount of BSA adsorbed on to the surface can be expressed simply as the  $[N]/[F]$  ratio. The dependence of the  $[N]/[F]$  ratio on the surface concentration of the grafted PEGMA polymer is summarized in Fig 10. Thus, even with the relatively low surface coverage by the poly(ethylene glycol) (PEG) chains, a significant reduction in BSA adsorption can be achieved. For the membrane with a surface  $[C]/[F]$  ratio of 2.5 and cast from the P(PEGMA)-*graft*-PVDF copolymer with a bulk graft concentration or  $[\text{PEGMA}]/[\text{CH}_2\text{CF}_2]$  ratio of 0.059, the amount of BSA adsorption is almost negligible.

Possible explanations for the passivity of the surface-immobilized PEG towards proteins include its minimum interfacial free energy in water, its hydrophilicity, its high surface mobility, and its steric stabilization effects, as well as its unique solution properties and molecular conformation in water.<sup>24</sup> Among the common water-soluble polymers, PEG is one of most flexible polymers in an aqueous medium because of the flexible ether linkages in its backbone and the absence of bulky side groups. Thus, it is sterically less hindered in the aqueous medium. The PEG molecule has a large excluded volume in water.<sup>12</sup> In an aqueous environment, the surface with flexible hydrated PEG chains and a large excluded volume

tends to repel protein molecules that approach the surface.<sup>25,26</sup> In addition, the PEG chains grafted onto the PVDF backbone can assume a brush-like microstructure and thus are dense and highly effective in repelling the protein molecules. These hydrodynamic characteristics help to account for the fact that the surface bearing PEGMA polymer molecularly grafted on the PVDF backbone is very effective in preventing protein adsorption.

### Conclusion

A new graft copolymer, P(PEGMA)-*graft*-PVDF, was successfully synthesized through the molecular graft copolymerization of PEGMA on to the ozone-activated PVDF backbone. The UF membranes prepared from this copolymer by the phase-inversion process in water showed enrichment of the hydrophilic PEGMA component in the surface region. The UF membranes with a graft concentration ( $[\text{PEGMA}]/[\text{CH}_2\text{CF}_2]_{\text{bulk}}$  ratio) greater than 0.06 were efficient in repelling protein adsorption. Thus, the new copolymer is a promising candidate for fabricating UF membranes with good anti-fouling properties.

### Acknowledgement

The authors are grateful to Mr Y. Zhang, Department of Physics, and Mr S. Li, Department of Chemical Engineering, National University of Singapore, for the XPS measurements.

### References

- 1 D. Wang, K. Li and W. K. Teo, *J. Membr. Sci.*, 1999, **163**, 211.
- 2 J. F. Hester, P. Banerjee and A. M. Mayes, *Macromolecules*, 1999, **32**, 1643.
- 3 K. J. Kim, A. G. Fane and C. J. D. Fell, *Desalination*, 1988, **70**, 229.
- 4 L. E. S. Brink, S. J. G. Elbers, T. Robbertsen and P. J. Both, *J. Membr. Sci.*, 1993, **76**, 281.
- 5 Y. Wang, J. H. Kim, K. H. Choo, Y. S. Lee and C. H. Lee, *J. Membr. Sci.*, 2000, **169**, 269.
- 6 M. Ulbricht and G. Belfort, *J. Membr. Sci.*, 1996, **111**, 193.
- 7 M. Ulbricht, K. Richau and H. Kamusewitz, *Colloids Surf., A*, 1998, **138**, 353.
- 8 H. Iwata, M. Oodate, Y. Uyama, H. Amemiya and Y. Ikada, *J. Membr. Sci.*, 1991, **55**, 119.
- 9 H. Iwata and T. Matsuda, *J. Membr. Sci.*, 1988, **38**, 185.
- 10 J. M. Shelton, I. M. Reed and C. R. Hawes, *J. Membr. Sci.*, 1991, **62**, 87.
- 11 T. J. Su, J. R. Lu, Z. F. Cui, B. J. Bellhouse, R. K. Thomas and R. K. Heenan, *J. Membr. Sci.*, 1999, **163**, 265.
- 12 J. H. Lee, H. B. Lee and J. D. Andrade, *Prog. Polym. Sci.*, 1995, **20**, 1043.
- 13 T. Fargere, M. Abdennadher, M. Delmas and B. Boutevin, *J. Polym. Sci., Part A: Polym. Chem.*, 1994, **32**, 1337.
- 14 *Methods of Chemical Analysis*, 2nd edn., Walton, Principles and Prentice-Hall, Englewood Cliffs, NJ, 1964; pp. 175–178.
- 15 H. Strathmann and K. Kock, *Desalination*, 1977, **21**, 241.
- 16 J. H. Lee, B. J. Jeong and H. B. Lee, *J. Biomed. Mater. Res.*, 1997, **34**, 105.
- 17 T. Wang, E. T. Kang, K. G. Neoh, K. L. Tan and D. J. Liaw, *Langmuir*, 1998, **14**, 921.
- 18 E. T. Kang, K. G. Neoh, K. L. Tan and F. C. Loh, *Synth. Met.*, 1997, **84**, 59.
- 19 B. Boutevin, J. J. Robin and A. Serdani, *Eur. Polym. J.*, 1992, **28**, 1507.
- 20 R. J. Good, *J. Am. Chem. Soc.*, 1952, **74**, 5041.
- 21 B. Boutevin, Y. Pietrasanta and J. J. Robin, *Eur. Polym. J.*, 1991, **27**, 815.
- 22 *Surface Analysis of Polymers by XPS and Static SIMS*, D. Briggs, Cambridge University Press, 1998, p. 65.
- 23 *High Resolution XPS of Organic Polymers: The Sienta ESCA Database*, G. Beamson and D. Briggs, John Wiley, 1992, p. 228.
- 24 R. Kjellander and E. Florin, *J. Chem. Soc., Faraday Trans. 1*, 1981, **77**, 2053.
- 25 J. Hermans, *J. Chem. Phys.*, 1982, **77**, 2193.
- 26 W. R. Gombotz, G. H. Wang, T. A. Horbett and A. S. Hoffman, *J. Biomed. Mater. Res.*, 1991, **25**, 1547.